

Optical spectroscopy of Er³⁺ and Yb³⁺ co-doped fluoroindate glasses

C. T. M. Ribeiro, A. R. Zanatta,^{a)} and L. A. O. Nunes

Instituto de Física de São Carlos, Universidade de São Paulo, P.O. Box 369, São Carlos, SP, 13560-970, Brazil

Y. Messaddeq

Instituto de Química de Araraquara, Universidade do Estado de São Paulo, P.O. Box 355, Araraquara, SP, 14800-970, Brazil

M. A. Aegerter

Institut für Neue Materialien, INM, D-66123 Saarbrücken, Germany

Optical absorption, Stokes, and anti-Stokes photoluminescence were performed on Er³⁺-Yb³⁺ co-doped fluoroindate glasses. For compounds prepared with a fixed 2 mol % ErF₃ concentration and YbF₃ contents ranging from 0 to 8 mol %, important *upconversion* processes were observed as a function of temperature and photon excitation energy. Based on the experimental data, two mechanisms for the *upconversion* (or anti-Stokes photoluminescence) processes were identified and analyzed in detail. At high Yb contents, the *upconversion* mechanisms are mostly determined by the population of the ²F_{5/2} levels of Yb³⁺ ions (or ⁴I_{11/2} levels of Er³⁺ ions, by energy transfer) regardless of the photon excitation energy and temperature of measurement. Moreover, green and red light emission have similar intensities when a large Yb³⁺ content is present.

I. INTRODUCTION

Over the last 25 years, the *upconversion* of infrared (IR) to shorter wavelengths of lanthanide ions in a wide range of glassy and crystalline hosts have been extensively studied due to their technological applications in the field of optical devices.^{1,2} Heavy-metal fluoride (HMF) glasses, in particular, have attracted considerable attention as favorable host materials for *upconversion* purposes. The lower vibrational frequencies of the HMF glasses minimize the nonradiative (multiphonon) relaxation of the excited lanthanide ions improving, in this way, the light emission. For practical reasons, Er³⁺-doped HMF compounds are the most interesting since they can be pumped by photons around 800–1000 nm, the wavelength region in which the most powerful diode lasers are presently available. In addition to the host-dependent radiative emission of these materials, the concentration of Er is also of great importance. At high Er contents the distance r between the Er³⁺ ions is small, and the electric dipole-dipole interactions between the different ions take place with a strength depending on r^{-6} .^{3,4} These interactions effectively lower the fraction of the excited Er³⁺ at a given pump power causing a reduction in the efficiency of light emission. In order to reduce these energy losses, special compounds have been studied either by means of special hosts⁵ or by investigating the effect of co-doping with different rare-earth ions.

With the above remarks in mind, a systematic study has been performed in a new class of rare-earth doped fluoride glasses. Er³⁺ and Yb³⁺ ions have been incorporated in a fluoroindate glassy matrix and their optical properties have

been studied. Both IR and *upconverted* visible (VIS) emission of light were investigated as a function of Yb concentration, temperature, and incident photon energy.

II. EXPERIMENTAL DETAILS

Er-containing fluoroindate glasses were prepared with different YbF₃ concentrations. All the glasses considered in this work presented a fixed 2 mol % of ErF₃ (the most efficient concentration for *upconversion* of green light)⁶ and YbF₃ contents ranging from 0 to 8 mol %. The glass compositions are reported in Table I. After mixture of the chemical precursors, the batch was heated in a Pt crucible at 800 °C during 1 h for melting and at 850 °C for fining. All the melting, fining, and preparation procedures were performed in a dry box under an Ar atmosphere (water vapor ≤ 10 ppm). After heating, the melt was cast into a preheated mold at ~250 °C and slowly cooled to room temperature. Finally, the samples were cut and polished in a parallelepiped shape with ~2 mm thicknesses. Optical absorption measurements were carried out at room temperature in the UV-VIS-NIR range using a Cary17 spectrophotometer. The emission spectra of Stokes and *upconverted* photoluminescence were achieved through standard optical setups. The Stokes photoluminescence setup employed the 488 nm line of an Ar⁺ laser, a Ge detector and *in-phase* techniques. *Upconversion* spectra were obtained using two different cw photon sources: at 790 nm from a Ti-sapphire solid state laser and at 980 nm from an AlGaAs diode laser. For these cases, the signals were detected by a photomultiplier tube (RCA 31034) connected to an electrometer. In both setups the emission components were separated by dispersive instruments: a 0.25 m Czerny–Turner type and a double 0.85 m monochromator

^{a)}Electronic mail: zanatta@ifqsc.sc.usp.br

TABLE I. Batch compositions employed for the preparation of InF_3 -based glasses. X denotes the concentration of YbF_3 ($X=0.2, 1, 2, 4,$ and 8 mol %). Single doped fluoroindate glasses (with ErF_3 2 mol % and with YbF_3 2 mol %) were also included.

Glass	InF_3	BaF_3	ZnF_2	SrF_2	GdF_3	NaF	ErF_3	YbF_3
Er	34	16	20	20	6	2	2	0
ErYbX	$36-X$	16	20	20	6	0	2	X
Yb	40	20	19	15	2	2	0	2

for light emission in the IR and VIS energy ranges, respectively. Radiative lifetimes were obtained from mechanically chopping the cw pumping beam (488 nm) and by signal averaging the resulting photoluminescence decay with a digital oscilloscope.

III. DATA ANALYSIS

A. Optical absorption

Figure 1 illustrates the absorption spectra at room temperature, in the 400–1700 nm wavelength range, obtained from glasses with different doping levels. In the considered IR energy range, Er^{3+} - and Yb^{3+} -co-doped glasses present various absorption features at: ~ 480 nm (${}^4I_{15/2} \rightarrow {}^4F_{7/2}$); ~ 530 nm (${}^4I_{15/2} \rightarrow {}^2H_{11/2}$); ~ 650 nm (${}^4I_{15/2} \rightarrow {}^4F_{9/2}$); ~ 975 nm (${}^4I_{15/2} \rightarrow {}^4I_{11/2}$), and ~ 1530 nm (${}^4I_{15/2} \rightarrow {}^4I_{13/2}$) corresponding to transitions due to Er^{3+} ions. On the other hand, glasses containing only Yb^{3+} ions, present a single peak at ~ 975 nm due to the ${}^2F_{7/2} \rightarrow {}^2F_{5/2}$ transition. Both ${}^4I_{15/2} \rightarrow {}^4I_{11/2}$ and ${}^2F_{7/2} \rightarrow {}^2F_{5/2}$ optical transitions associated

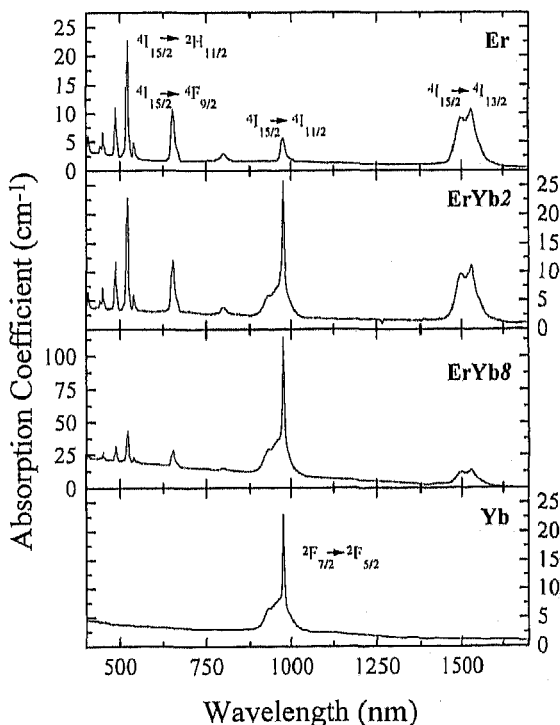


FIG. 1. Room temperature absorption spectra in the 400–1700 nm wavelength range of fluoroindate glasses prepared with different ErF_3 and YbF_3 concentrations. The absorption coefficient at ~ 975 nm increases at higher Yb contents. The most important absorption bands are identified.

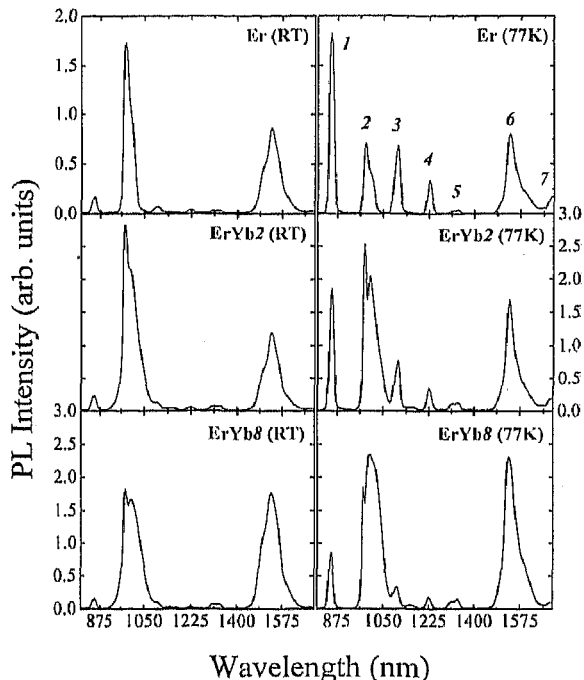


FIG. 2. Stokes photoluminescence spectra at two different temperatures of Er^{3+} and Er^{3+} - Yb^{3+} -doped fluoroindate glasses. The emissions identified in the figure correspond to either indirect (1, 3, 4, and 7) or direct (2 and 6) optical transitions. The structure at ~ 1350 nm (transition 5) is probably associated to some nonintentional contamination during the glasses preparation.

to Er^{3+} and Yb^{3+} ions, respectively, occur at the same wavelength, and as can be seen from Fig. 1, present an absorption coefficient that increases with the Yb content. A rough estimation indicates that the absorption coefficient near ~ 975 nm due to the Yb^{3+} ions is a factor of four times greater than those exhibited by the Er^{3+} ions.

B. Stokes photoluminescence

Figure 2 displays the IR photoluminescence spectra at room and liquid nitrogen temperatures of fluoroindate glasses prepared with a fixed 2 mol % of ErF_3 concentration and YbF_3 contents of 0, 2, and 8 mol %. Some of the observed emissions were identified by numbers in the figure and correspond to either direct (2 and 6) or indirect (1, 3, 4, and 7) transitions. These emission features correspond to the following transitions: 1 at ~ 850 nm (Er^{3+} , ${}^4S_{3/2} \rightarrow {}^4I_{13/2}$); 2 at ~ 980 nm (Er^{3+} , ${}^4I_{11/2} \rightarrow {}^4I_{15/2}$, and Yb^{3+} , ${}^2F_{5/2} \rightarrow {}^2F_{7/2}$); 3 at ~ 1100 nm (Er^{3+} , ${}^4F_{9/2} \rightarrow {}^4I_{13/2}$); 4 at ~ 1230 nm (Er^{3+} , ${}^4S_{3/2} \rightarrow {}^4I_{11/2}$); 5 at ~ 1350 nm (probably due to some contamination); 6 at ~ 1540 nm (Er^{3+} , ${}^4I_{13/2} \rightarrow {}^4I_{15/2}$), and 7 at ~ 1650 nm (Er^{3+} , ${}^4I_{9/2} \rightarrow {}^4I_{13/2}$). At lower temperatures there is a reduction of the number of nonradiative processes and, as a consequence, all the indirect transitions can be easily detected.

C. Anti-Stokes photoluminescence (upconversion)

The light emission spectra in the VIS energy range of glasses ErYb2 and ErYb8 (see Table I) measured under photon excitations of 790 and 980 nm at two different tempera-

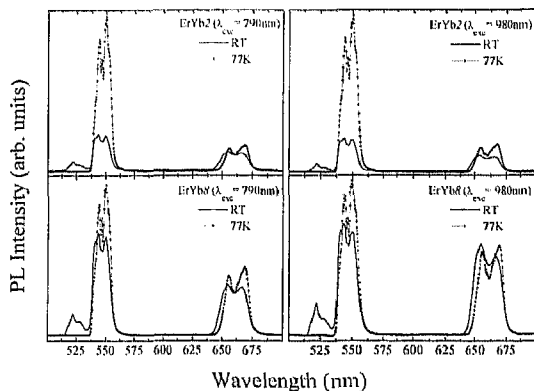


FIG. 3. Anti-Stokes photoluminescence for the glasses ErYb2 and ErYb8 excited by photons with wavelengths of 790 and 980 nm. At room temperature three main emissions can be observed: at 525 nm (${}^2H_{11/2} \rightarrow {}^4I_{15/2}$), at 545 nm (${}^4S_{3/2} \rightarrow {}^4I_{15/2}$), and at 660 nm (${}^4F_{9/2} \rightarrow {}^4I_{15/2}$).

tures are displayed in Fig. 3. Two main structures are present for both excitation sources: at ~ 545 nm and ~ 660 nm corresponding to the Er^{3+} ions ${}^4S_{3/2} \rightarrow {}^4I_{15/2}$ and ${}^4F_{9/2} \rightarrow {}^4I_{15/2}$ optical transitions, respectively. At room temperature, a third feature is observed and is associated to the ${}^2H_{11/2} \rightarrow {}^4I_{15/2}$ transition in Er^{3+} ions. At 77 K, however, the intensity of this transition is drastically reduced since the ${}^2H_{11/2}$ level is thermally populated.⁷ Another interesting aspect observed in the present glasses is related to the Yb^{3+} concentration: glasses with a high content of Yb^{3+} exhibit green (~ 545 nm) and red (~ 660 nm) light emission with similar intensity. It may be noted that, irrespective of the temperature of measurement, the intensity of both green and red emissions are comparable in the ErYb8 glass when pumped by photons with 980 nm contrary to the behavior displayed by single Er^{3+} -doped fluorindate hosts.⁸

IV. DISCUSSION

For the glasses being discussed here and within the analyzed range of concentrations, the absorption coefficients at ~ 975 nm scale linearly with the Yb^{3+} content. It is worth mentioning that most of the radiative transitions in the IR

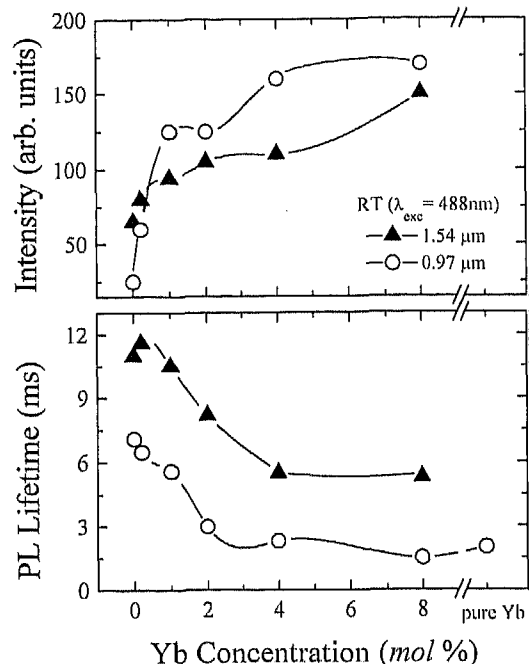


FIG. 4. Representation of the integrated intensity and the radiative lifetimes of the transitions at ~ 980 nm and ~ 1540 nm as a function of the Yb^{3+} concentration (ErYbX glasses). These data were obtained at room temperature and under 488 nm photon excitation. Yb^{3+} contents larger than ~ 4 mol % do not cause great changes in both the intensity and lifetimes. The lines drawn through the points are guides for the eyes.

energy range is also dependent on the Yb^{3+} concentration. Figure 4 displays the integrated intensity and the radiative lifetime associated to the optical emissions at 980 and 1540 nm observed at room temperature. Significant changes in these emissions can be observed for samples containing Yb^{3+} ions up to ~ 4 mol %. This fact can be understood based on the number of available rare-earth centers: for a fixed concentration of Er^{3+} (2 mol %), more Yb^{3+} ions increase the optical absorption and, consequently, the probability of radiative emission. Yb^{3+} contents larger than 4 mol %, do not cause great modifications specially in the radiative lifetimes. It is also evident from Fig. 4 that, for Yb^{3+} con-

TABLE II. Upconversion power law coefficient n observed after a $\log\text{-}\log I_{vis}$ vs I_{IR} representation for several vitreous matrices. As can be seen, different mechanisms occur for the red, green, and blue light emissions depending both on the photon excitation source and the glassy matrix. The last three matrices were simultaneously doped with Er^{3+} and Yb^{3+} ions.

Vitreous matrix	λ_{exc} (nm)	Power law			Ref. No.
		~ 650 nm	~ 550 nm	~ 410 nm	
Phosphate	1064	1.89	1.96	...	10
Oxide	797	...	1.5	...	11
Chloride	800	...	1.5	2	12
Fluoride	800	1.5-2	2	...	13
Fluoride	1500	1.97	1.98	...	14
Fluorozirconate	1130 and 1500	2.01	2.6	2.8	15
Fluoroindate	647	...	1.5-1.7	1.6-1.9	6
Fluoroindate	790	1.6	2.1	2.9	8
Fluorohafnate	974	1.94	1.93	...	7
Fluoroindate	790	2.11	2.14	...	this work
Fluoroindate	980	2.07	2.18	...	this work

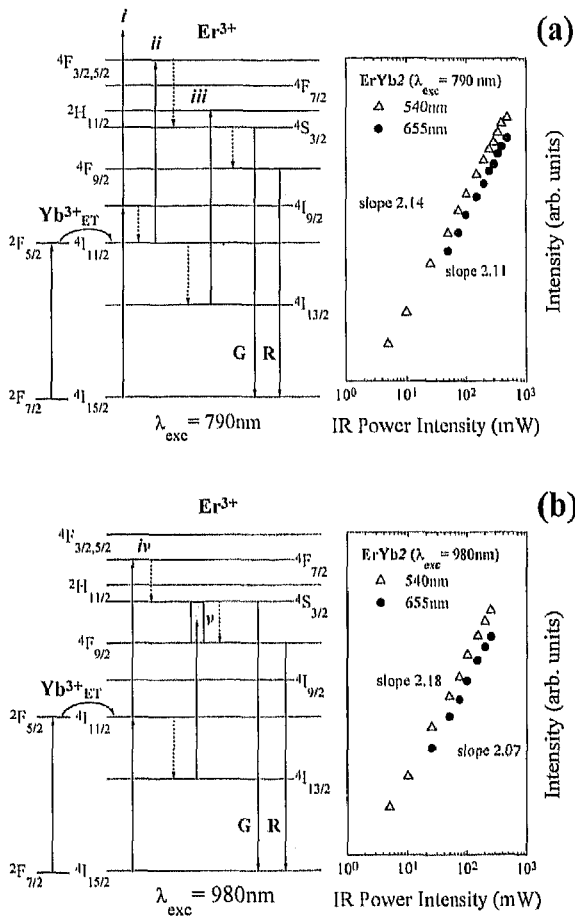


FIG. 5. Schematic energy levels diagram of the Er^{3+} and Yb^{3+} ions (left-hand side) and power law (right-hand side) for *upconversion* of light in the ErYb_2 fluorindate glass. (a) Corresponds to data taken under 790 nm photon excitation and (b) stands for 980 nm pumping. Excitation is represented by means of thick upward arrows; broken downward arrows indicate de-excitation processes and thin downward arrows with labels G and R correspond to green and red emissions, respectively. As represented in the figure, energy transfer (ET) can occur between the $^2F_{5/2}$ and $^4I_{11/2}$ levels of the Yb^{3+} and Er^{3+} ions.

concentrations larger than ~ 4 mol %, the radiative lifetime associated with the transition at 980 nm is the same as that presented in single Yb^{3+} -doped fluorindate glasses.

For optimization purposes of the IR upconverted radiation in HMF glasses it is important to identify the excitation and the de-excitation mechanisms. For any process of *upconversion* of light, the visible output intensity I_{VIS} of the compound is proportional to some power n of the infrared excitation intensity I_{IR} , i.e., $I_{\text{VIS}} \propto (I_{\text{IR}})^n$. In a log-log representation of I_{VIS} vs I_{IR} the angular slope coefficient n indicates the number of IR absorbed photons per photon emitted in the VIS. These absorption-emission mechanisms depend strongly not only on the pumping wavelength (which determines the pumped energy level) but also on the glassy matrix.⁹ To illustrate these particular features, Table II presents the *upconversion* power law exhibited by several glasses under different photon excitation.

Figures 5(a) and 5(b) show, on the left-hand side, a schematic diagram of the energy levels of Er^{3+} and Yb^{3+} ions as well as some possible mechanisms present in the process of

upconversion of light. The power law observed in the ErYb_2 glass was represented on the right-hand side of Figs. 5(a) and 5(b) for two different IR photon sources. Based on these energy diagrams and on the spectroscopic data, some aspects related to the *upconversion* in these fluorindate glasses can be derived:

(a) According to the value of n obtained from the power law, both the green (~ 545 nm) and red (~ 660 nm) radiation originate from processes involving two photons ($n \sim 2$); (b) taking into account the radiative lifetimes, energy levels, and pumping energy, the green radiation can have its origin from the two-photon-assisted mechanisms indicated in Figs. 5(a) and 5(b) by the labels *i*, *ii*, *iii*, *iv* and *v*; (c) the red emission originates from the $^4F_{9/2}$ level that can be populated via deexcitation of the $^4S_{3/2}$ level. When pumped by photons of 980 nm, the mechanism *v* is also probable. Note that in spite of the absence of states between the $^4S_{3/2}$ and $^4F_{9/2}$ energy levels, there is a considerable absorption coefficient at these wavelengths due to the glassy host (see Fig. 1); (d) at low Yb^{3+} contents, the green radiation is more temperature dependent, and is associated with an increase in the population of the $^4S_{3/2}$ level;⁸ (e) when pumped by 980 nm photons, and at high Yb^{3+} concentrations, the most striking feature is associated to the relative intensity of the green and red emissions. Moreover, the intensity of green light does not present a great dependence with temperature. It seems that the increase of the population of the $^4I_{11/2}$ (or $^2F_{5/2}$) is the preponderant factor for the *upconversion* mechanisms. If this is true, the Yb^{3+} ions can be viewed as a buffer level that drastically increases the probability of excitation from the $^2F_{5/2}$ level (or $^4I_{11/2}$, by energy transfer-ET).

V. CONCLUSIONS

Looking for efficient light emitters, Er^{3+} and Yb^{3+} ions were introduced in fluorindate hosts and several optoelectronic properties were analyzed in detail. Both IR and *upconverted* VIS emission of light were investigated as a function of Yb^{3+} concentration, temperature, and incident photon energy. For a fixed 2 mol % concentration of Er^{3+} ions, the Yb^{3+} content determines several interesting features and two mechanisms for the *upconversion* phenomena in these HMF glasses were identified. Within the analyzed range of rare-earth concentrations the absorption coefficients at ~ 975 nm scale linearly with the Yb^{3+} content. As a consequence, the intensity of the observed radiative transitions, both Stokes and anti-Stokes, scales with the Yb^{3+} content and an enhancement of a factor of 4 or 5 could be achieved. At high Yb^{3+} concentrations, the *upconversion* processes are mostly determined by the population at the $^2F_{5/2}$ level (or $^4I_{11/2}$ level, by energy transfer) regardless of the excitation photon energy. Contrary to the single Er^{3+} -doped fluorindate glasses, at high Yb^{3+} concentrations these compounds present comparable green and red light intensities.

ACKNOWLEDGMENTS

This work was supported by the Brazilian Agencies CNPq and FAPESP.

- ¹F. E. Auzel, Proc. IEEE **61**, 758 (1973).
- ²J. C. Wright, in *Radiationless Process in Molecules and Condensed Phases*, Vol. 15. of Topics of Applied Physics, edited by F. K. Fong (Springer, New York, 1976), p. 239.
- ³I. M. Rosman, in *Luminescence of Crystals, Molecules and Solutions*, edited by F. Williams (Plenum, New York, 1973), p. 324.
- ⁴Ch. Buchal, Th. Siegrist, D. C. Jacobson, and J. M. Poate, Appl. Phys. Lett. **68**, 438 (1996).
- ⁵G. Nycolak, P. C. Becker, J. Shmulovich, Y. H. Wong, D. J. DiGiovanni, and A. J. Bruce, IEEE Photonics Technol. Lett. **5**, 1014 (1993); G. Nycolak, M. Haner, P. C. Becker, J. Shmulovich, and Y. H. Wong, IEEE Photonics Technol. Lett. **5**, 1185 (1993).
- ⁶R. Reiche, L. A. O. Nunes, C. C. Carvalho, Y. Messaddeq, and M. A. Aegerter, Solid State Commun. **85**, 773 (1993).
- ⁷See, for example, M. A. Chamarro and R. Cases, J. Lumin. **46**, 59 (1990).
- ⁸T. Catunda, L. A. O. Nunes, A. Florez, Y. Messaddeq, and M. A. Aegerter, Phys. Rev. B **53**, 6065 (1996).
- ⁹H. Kuroda, S. Shionoya, and T. Kushida, J. Phys. Soc. Jpn. **1**, 125 (1972).
- ¹⁰Y. L. Lu, Y.-Q. Lu, and N. B. Ming, Appl. Phys. B **62**, 287 (1996).
- ¹¹B. R. Reddy and P. Venkateswarlu, Appl. Phys. Lett. **64**, 1327 (1994).
- ¹²M. Shojiya, M. Takahashi, and K. Kadono, Appl. Phys. Lett. **65**, 1874 (1994).
- ¹³E. Oomen, P. LeGall, and A. Dongen, J. Lumin. **46**, 353 (1990).
- ¹⁴D. C. Yeh, I. Schneider, R. S. Afzal, and I. Aggarwal, J. Appl. Phys. **69**, 1648 (1990).
- ¹⁵S. C. Goh, J. Non-Cryst. Solids **161**, 227 (1993).